engineering proceedings

Type of the Paper (Proceedings, Abstract, Extended Abstract, Editorial, etc.)

Electrical Characterization of Cu-Doped PEDOT: PSS Polymeric Thin Films

Ameneh Mikaeeli[1,2,*], Nathan Jukam[2], Robert Szczesny[3], Arne Ludwing[2], Ismail bolukbasi[2], Andreas D. Wieck[2], and Michal Pawlak[2]

[1] Institute of Physics, Faculty of Physics, Astronomy, and Informatics, Nicolaus Copernicus University in Torun, Grudziadzka 5, 87-100 Torun, Poland; ameneh.mikaeeli@doktorant.umk.pl (A. M.); mpawlak@fizyka.umk.pl (M.P.)

[2] Chair of Applied Solid-State Physics, Faculty of astronomy and Physics, Ruhr-University Bochum, D-44780, Bochum, Germany; ameneh.mikaeeli@ruhr-uni-bochum.de (A. M); nathan.jukam@rub.de (N. J.); arneh.ludwing@rub.de (A. L.); ismail.boeluekbasi@ruhr-uni-bochum.de (I. B); andreas.wieck@rub.de (A. D. W.)

[3] Faculty of Chemistry, Nicolaus Copernicus University in Torun, Gagarina 7, 87-100 Torun, Poland; roszcz@umk.pl (R. S.)

* Correspondence: ameneh.mikaeeli@doktorant.umk.pl

Abstract: In this study we investigate the electrical properties in the transparent conductive polymer poly(3,4-ethylendioxythiophene):poly(styrene sulfonate) (PEDOT:PSS) and Cu-doped (PEDOT: PSS 1.3% + $CuCl_2$) using Hall measurements in the van der Pauw configuration. The influence of the doping on the electrical conductivity, Hall mobility, and carrier concentration is demonstrated in Cu-PEDOT:PSS and compared with pure PEDOT:PSS. However, we figured out the difficulties for making Cu-doped polymers. The sheet resistance was measured to determine electrical conductivity, aided by knowledge of the thin film thickness. Temperature dependency was evaluated using a closed cycle cryostat, covering temperatures ranging from 8K to 300 K. These comprehensive measurements provide valuable insights into the electrical behavior and temperature characteristics of PEDOT:PSS and PEDOT: PSS 1.3% + $CuCl_2$, facilitating the development of high-performance organic electronic devices.

Keywords: conductive polymer; PEDOT: PSS; electrical conductivity; Hall measurements

1. Introduction

Conducting polymers have emerged as a fascinating class of materials, offering a bridge between traditional inorganic semiconductors and organic compounds. Among these materials, poly(3,4-ethylenedioxythiophene):poly(styrene sulfonate), (PEDOT:PSS), is a most famous p-type conductive polymer which exhibits promising properties, such as high transparency in the visible range, flexibility, and compatibility with solution-based processing methods, making it a candidate for a wide array of thermoelectric applications [1-4]. It's a hole transport material which structured with a hydrophobic, conductive PEDOT surrounded by an insulating, hydrophilic PSS chain [5]. However, the pristine PEDOT:PSS film derived from its aqueous solution, typically exhibits a low electrical conductivity (< 1 S/cm). This diminished conductivity is due to the presence of the insulating PSS moiety, which is crucial for the formation of aqueous dispersion required for solution processing. In 2002, Kim et al. pioneered conductivity enhancement in PEDOT:PSS by doping the PEDOT:PSS aqueous solution with small-molecule organic compounds such as polar solvents dimethyl sulfoxide (DMSO) or dimethylformamide (DMF) into [6]. Since then, various techniques have been reported to enhance PEDOT:PSS conductivity, with recent findings showing it can exceed 3000 S/cm [7]. Moreover, conductivity enhancement through treatment with different salts aqueous solutions including metal ions like $CuCl_2$

is another way of interest. The metal ion and anion can lead to conformational change of the PEDOT:PSS chains in accordance with loss of PSS from the polymer [8-10]. Besides, effect understanding the temperature dependency of PEDOT:PSS is essential for optimizing its functionality in various applications, as it directly impacts the material's electrical and thermal performance, complementing the significance of doping techniques.

In this paper, we present an analysis of the temperature-dependent behavior of PEDOT:PSS and the problems revealing for doping PEDOT:PSS with $CuCl_2$ like the resultant inhomogeneous solutions, the stability of the final polymers on the glass as well as cleaving problems. Our investigation employed Hall measurements conducted using the Van der Pauw configuration.

2. Materials and Methods

2.1. Hall Measurements

The Van der Pauw configuration was used for Hall effect measurements of the studied samples. Figure 1 shows the schematic of the set up for Hall measurements. The current applied from contacts 1 to 3 and the hall voltage gained between contacts 2 and 4. The measuring current was supplied by a DC source (Keithley 220). The digital multimeter served as the voltage measurement device (Keithley 2700). With an accuracy of 6½ digits and a voltage resolution of 100 nV, this setup enables highly precise measurements for both very low and high-resistance samples and, due to its high input resistance (> 10 GΩ). For the temperature sweep, the sample was placed in the closed cycle cryostat with the applied magnetic field (0.28T). All the devices are connected to PC via a GPIB cable and then reading the data via Labview program [8].

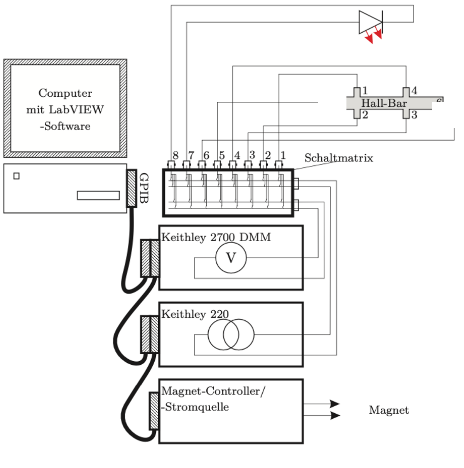

Figure 1. Schematic of the DC Hall setup: For measurements under gate bias, an additional voltage source (Keithley 236) is used (not shown here). In addition, measurements with the pulse cryostats from Brücker involve a temperature controller and Gaussmeter [8].

2.2. Conductivity measurement Based on Hall Measurements

The Hall effect is based on the fundamental principle of the Lorentz force. When an electron moves perpendicular to an applied magnetic field while traveling along an electric field, it experiences a magnetic force $(-qv \times B)$ acting in a direction perpendicular to both fields. The resulting Lorentz force, F, can be described as $-q(E + v \times B)$.

Under these conditions, a constant current (I) flows along the x-axis, accompanied by a z-directed magnetic field. Electrons, influenced by the Lorentz force, shift towards the negative y-axis, creating an excess negative surface charge and producing the Hall voltage (V_H) across the sample. By measuring the Hall voltage once can measure the sheet density ($n_s = {}^{IB}/_{q|V_H|}$). Ultimately, if the layer thickness is known it is possible to measure resistivity ($\rho = R_s d$) and subsequently the electrical conductivity ($\rho = {}^{1}/_{\sigma}$) [12].

2.2. Sample Preparation

The chemical structure of the PEDOT:PSS is shown in Figure 2. In comparison to other conductive polymers PEDOT:PSS is stable both in water and ambient due to the formation of a reliable polycomplex between PEDOT and PSS where PSS acts as both a chemical dopant and an emulsifier [9].

The deposition of polymers onto glass substrates (15x15 mm) was carried out using the spin-coating technique (Spin Coater Laurell 650SZ). Prior to the deposition process, the glass substrates underwent a thorough cleaning procedure involving sequentially rinsing in an ultrasonic bath for 5 minutes each, first with acetone, followed by ethanol, and finally with deionized water. Subsequently, the rinsed substrates were left to air dry under ambient conditions. Firstly, PEDOT: PSS 3-4 % in water was filtered through a 0.45 µm syringe filter. Then 200 µl of pure PEDOT:PSS has been deposited on the glass substrate and then spun with a speed of 4000 rpm. Secondly, PEDOT: PSS 1.3% + $CuCl_2$ was filtered through a 0.45 µm syringe filter and $CuCl_2xH_2O$ was added (2 mg of copper salt/1.17 ml PEDOT:PSS). The solution was ultrasonicated for 5 min before deposition. Then the 200 µl of solution was deposited on the glass substrate at a speed of 4000 rpm. Finally, all prepared samples have been dried using a heating plate at 110 °C for 15 min. However, for the conductivity measurements the samples have been cleaved to the 4x4 mm before placing in the closed cycle cryostat.

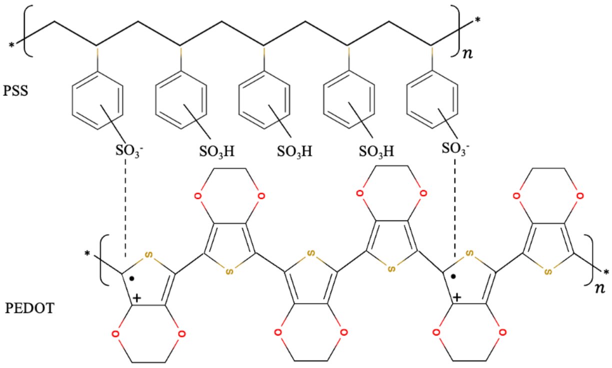

Figure 2. The chemical structure of the PEDOT:PSS.

2.3. Temperature Depenence on Electrical Conductivity

There are differennt models to investigate the temerature dependency of electrical conductivity of conductive polymers. Here we use two Mott and Schaefer–Siebert–Roth models for fitting the experimental data respectively.

2.3.1. Mott Model

This model is used to elucidation the temperature-dependent characteristics of distorted systems. In this model, charge carriers transition between distinct localized energy states of varying energy levels is based on absorbing phonon energy. Equation 1 shows the temperature dependency of electrical conductivity [10]:

$$\sigma = \sigma_0 exp\left[-\left(\frac{T_0}{T}\right)^{1/n+1}\right], \quad (1)$$

here n is the dimensionality of charge transfer, σ_0 is conductivity at room temperature and T_0 is Mott's temperature constant.

2.3.2. Schaefer–Siebert–Roth model

In this model, cnotrast to the Mott model the localization lengths and conjugation lengths are considered. Doping polymers with p or n dopants breaks p-bonds, resulting in charge carriers like polarons and bipolarons. These carriers, in turn, alter the conjugation lengths within the polymer backbone:

$$\sigma = \sigma_0 exp\left[-\left(\frac{T}{T_0}\right)^{-\gamma}\right] \text{ where } \frac{1}{4} < \gamma < \frac{1}{2}, \quad (2)$$

here σ_0 and T_0 depend upon localization length, and γ depends upon the density of states at the Fermi level.

3. Results and Discussion

3.1. Atomic Force Microscope (AFM)

The topology studies of polymeric thin films deposited on a glass substrate were measured by the Atomic Force Microscope (AFM) (Park Systems NX20). The obtained images provide information including variations in the surface roughness along the examined samples. The device contains a PPP-NCHR 5mm tip operating in a noncontact mode in the air at room temperature. Figure 3 displays AFM images of thin films a) PEDOT:PSS and b) PEDOT:PSS +$CuCl_2$. As can be seen in Table 1 the samples have smooth surface with roughness parameters values ranging from 1.43 – 6.23 nm and 1.89 – 2.9 nm for R_a and R_q respectively. Upon treatment with the $CuCl_2$ solution, the image analysis reveals a notable increase in surface roughness, accompanied by the emergence of prominent domains. This morphological transformation observed in the PEDOT:PSS film strongly indicates a significant conformational change in the polymer chains during the treatment.

Table 1. Values of roughness parameters (R_a and R_q) for samples.

Roughness parameter	**PEDOT:PSS 3-4%**	**PEDOT: PSS 1.3%+ $CuCl_2$**
R_a(nm)	6.23	1.43
R_q(nm)	2.90	1.89

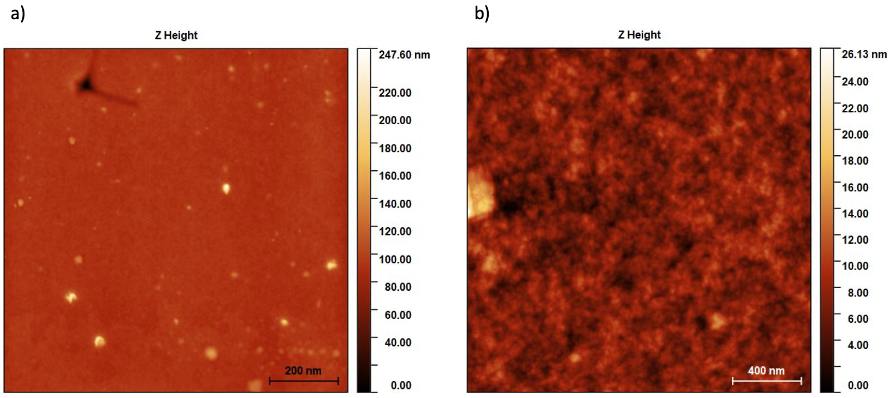

Figure 3. Surface morphology for the conductive polymers a) PEDOT:PSS and b) PEDOT:PSS 1.3%+CuCl2 obtained with atomic force microscope (AFM).

3.2. Conductive Atomic Force Microscope (C-AFM)

Besides the topology investigations, the C-AFM (Figure 4. a) Pure PEDOT:PSS, b) PEDOT: PSS 1.3% + $CuCl_2$) is performed for the two studied samples. Unexpectedly, the introduction of copper as a dopant led to a reduction in both current flow and sample conductivity, challenging the conventional assumption that the addition of metals uniformly enhances conductivity. Our measurements indicate that the pure polymer PEDOT:PSS (3-4%) exhibits notably higher conductivity than its copper-doped counterpart. This result emphasizes the variability in the impact of metal incorporation on sample conductivity, and it highlights the importance of careful consideration when introducing metals for conductivity enhancement.

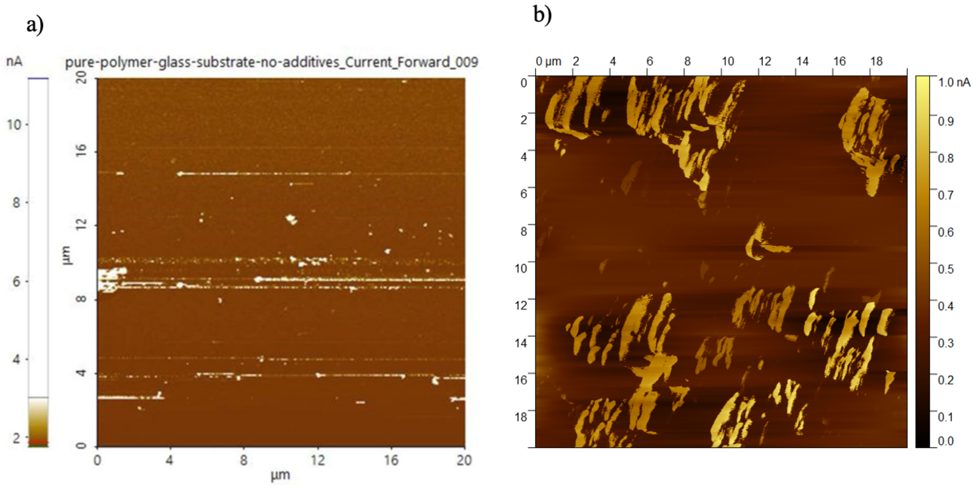

Figure 4. Current flow images for the conductive polymers a) PEDOT:PSS and b) PEDOT:PSS 1.3%+$CuCl_2$ obtained with conductive atomic force microscope (C-AFM).

3.3 Temperature Dependance Results

Figure 5 shows the results for temperature dependence of the electrical conductivity for PEDOT:PSS obtained from Mott and Roth models. It can be seen from both methods that there is a good correlation between electrical conductivity and the temperature, which it increase by increasing the temperature. Furthermore, the Roth model demonstrates superior performance in accurately representing the experimental data, possibly owing to its incorporation of the localization length with the conjugation length.

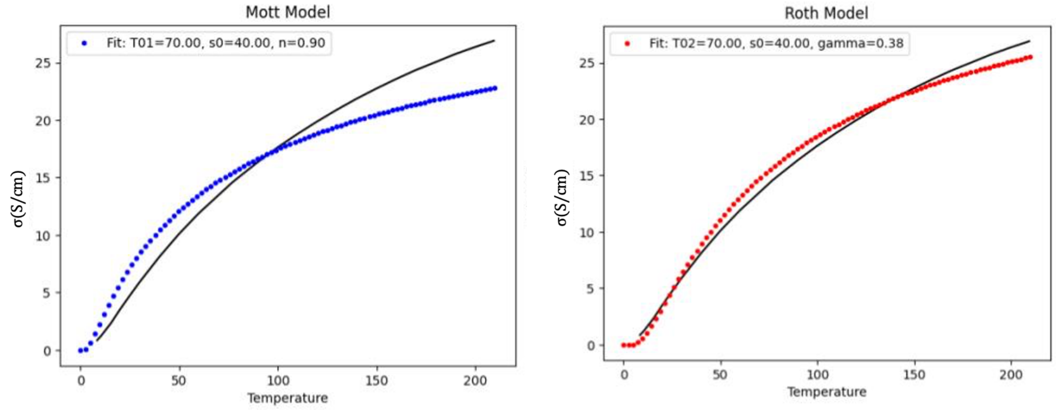

Figure 5. Temperature dependence of the electrical conductivity of PEDOT:PSS 3.4% water measured by closed cycle cryostat from 8K to 200K.

3.4 Hall Mobility and Carrier Concentration Density

Table 2 illustrates the related Hall mobility and sheet carrier density for the PEDOT:PSS at room temperature which is in agreement with literature.

Table 2. Values of Hall mobility and sheet carrier density (N2d) for PEDOT:PSS

Current (µA)	N2d (cm^2)	Mobility (cm^2/Vs)
3	2.89*10^15	2.37

4. Conclusion

In this study, we examined the temperature dependence of the conductive polymer PEDOT:PSS through Hall measurements employing the Van der Pauw configuration. Our findings revealed a significant temperature-dependent increase in the electrical conductivity of pure PEDOT:PSS. However, when investigating Cu-doped PEDOT:PSS, we encountered notable challenges that hindered our assessment of temperature dependency. These challenges included the lack of homogeneity in the final solution of PEDOT:PSS mixed with $CuCl_2$, possibly stemming from chemical incompatibility, polarity disparities, limited solubility, which may lead to phase separation or aggregation results in a non-homogeneous mixture. Additionally, cleaving the thin film after deposition on the substrate may have compromised its integrity, and the conductive silver paste used could potentially have dissolved the thin film due to its composition.

References

1. Pasha, A.; Roy, A. S.; Murugendrappa, M. V.; Al-Hartomy, O. A.; and Khasim, S. Conductivity and dielectric properties of PEDOT-PSS doped DMSO nano composite thin films *J. Mater Sci: Mater Electron*, **2016** *27*, 8332-8339.
2. Dong, J.; and Portale, G. Role of the solvent on the electrical conductivity of PEDOT:PSS *Adv. Mater. Interfaces,* **2020** *7,* 2000641.
3. Ahmad Shahrim, N. A.; Ahmad, Z.; Wong Azman, A.; Fachmi Buys, Y.; and Sarifuddin, N. Mechanisms for doped PEDOT:PSS electrical conductivity improvement *Mater. Adv.* **2021** *2*, 7118-7128.
4. Hui, S.; Congcong, L.; Qingling, J.; and Jingkun, X.; Effective approaches to improve the electrical conductivity of PEDOT:PSS: A review *Adv. Electron. Mater.* **2015** *1,* 1500017.
5. Sato, R.; Wasai, Y.; Izumi, Y., Ueno, K.; and Hajime, Influence of effective mass on carrier concentration for PEDOT:PSS and S-PEDOT thin films studied by ellipsometry and Hall measurement *J. Phys. Chem. C* **2023** 127, 13197-13206.
6. Kim, J.Y.; Jung, J.H.; Lee, D.E.; and Joo, J. Enhancement of electrical conductivity of poly(3,4-ethylenedioxythiophene)poly(styrene sulfonate by a change of a solvent *Synth. Mat.* **2002** 126, 311-316.
7. Xia, Y.; Sun, K.; and Ouyang, J. Solution metallic conducting polymer films as transparent electrode of optoelectronic devices *Adv. Mater.* **2012** 24, 2436.
8. Xia, Y.; High conductive (PEDOT:PSS) thin films and their application I polymer photovoltaic devices. Master Thesis, National University of Singapore, Singapore, 2011.
9. Xiong, C.; Qu, H.; Chen, W.; Zhang, L.; Qiu, L.; Zheng, L.; Xia, F. Real time detection of Cu(II) with PEDOT:PSS based organic electrochemical transistors. *Sci. China Chem*. **2017** 60, 1205-1211.
10. Rueda, J. D. M.; Diego, J.; Study of electrochemical synthesis of a hybrid material of poly (3,4-ethylenedioxy-thiophene) modified with copper species. Master Thesis, Universidad de Los Andes, Colombia, 2016.
11. Schulte-Braucks, C. H. Einfluss von Licht und Gate-Spannung auf Dichte und Beweglichkeit von niederdimensionalen Halbleiter-Strukturen. Master Thesis, Ruhr-University Bochum, Germany, 2013.
12. National Institute of Standards and Technology (NIST), https://www.nist.gov/pml/nanoscale-device-characterization-division/popular-links/hall-effect/hall-effect.
13. Sun, K.; Zhang, S.; Li, P.; Xia, Y.; Zhang, X.; Du, D.; Isikgor, F. H.; and Ouyang, J. Review on application of PEDOTs and PEDOT:PSS in energy conversion and storage devices *J. Mater. Sci.: Mater. Electron.* **2015** 26, 4438-4462.
14. Namsheer, K.; and Sekhar Rout, C. Conducting polymers: a comprehensive review on recent advances in synthesis, properties and applications *RSC Adv.* **2021** 11, 5659.